GANIL

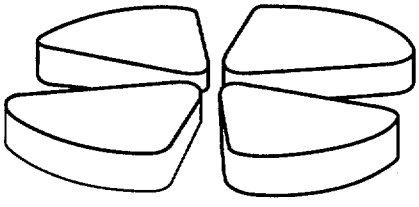

RIB production with high energy neutrons from Be(d,xn) reactions

D. Ridikas and W. Mittig

GANIL, BP 5027, F-14076 CAEN Cedex 5, France

July 3, 1998

GANIL P 98 22

RIB production with high energy neutrons from Be(d,xn) reactions

D. Ridikas and W. Mittig

GANIL, BP 5027, F-14076 CAEN Cedex 5, France

July 3, 1998

Abstract

An efficient way to produce the neutron-rich nuclei in the mass range of $70<A<170$ may be achieved via neutron induced fission in uranium ^{238}U. Depending on the incident neutron energy, the target size and its constituents, it might be also possible to increase this production rate by the secondary neutrons from primary fissions. A few different methods for producing neutrons and their induced fissions following the Be(d,xn) reactions are investigated within the SPIRAL Phase-II project at GANIL. Density, size and material contents of the production target as well as energy of the incident deuteron beam are the major parameters of interest. The production of neutron-rich isotopes presented seems to be very promising if compared to already existing or planned different RIB facilities.

1 Introduction

Together with an increase in the accelerator power available, the new radioactive ion beam (RIB) targets will have to be designed to deal with high power densities. This is a problem of concern to a number of RIB facility concepts currently under consideration at various laboratories world wide. One effective solution to this problem, as initially proposed by the Argonne National Laboratory group [1], is to decouple the heat dissipation issue from that of nuclide production and release to the ion source. This can be achieved by stopping primary beam in a

target-converter to produce an intense flux of secondary neutrons to irradiate a secondary production target located behind the first one.

The use of primary projectiles such as deuterons and light target materials as converters like beryllium seems to be the most efficient way to produce the most energetic and the most forward peaked neutrons. Deuterons also give the highest neutron yield from light targets if compared to proton or alpha induced reactions (see [2, 3] for detailed analysis).

Since the maximum yield of neutron-rich isotopes is achieved via neutron induced fission on uranium, the secondary production target could be uranium carbide or liquid uranium. Depending on its actual size, it is also possible to take advantage of the reactions induced by the secondary neutrons from primary fission reactions. For the production of a narrower range of neutron-rich nuclei near the peaks in the fast-neutron (1-4MeV) induced fission, it may be better to use lower energy neutrons produced by stopping the deuterons or protons in the ^{238}U or ^{184}W stopping target and have these neutrons induce fission in the secondary ^{238}U or higly enriched uranium (>50% ^{235}U) production target.

The prediction of production rates of radioisotopes rely heavily on existing computer codes, and it is essential to compare the results to available experimental data. The LAHET+PHT codes [4] are briefly described in Chapter 2. The benchmarking calculations for a number of typical data sets are presented in Chapter 3. Chapter 4 deals with a combined target assembly and model-based predictions of the RIB production in the experimental configuration as discussed above. The results are compared to the RIB intensities at already existing or planned different experimental facilities. Finally, the beam heating and cooling of thick targets for in-target production of exotic nuclei is discussed in Chapter 5.

2 The LAHET and PHT codes

The LAHET 2.70 code [4] employs the intranuclear cascade (INC) and evaporation models (EVAP), and includes two models of fission induced by high energy interactions: the ORNL model by Alsmiller et al. [5] and the RAL model by Atchison [6]. The fission models are employed with the evaporation model of Dresner [7]. The Fermi breakup model [8] is used for the disintegration of light nuclei ($A \leq 17$). LAHET also contains the multistage preequilibrium exciton model (MPM) as described in [9].

The photon transport (PHT) code [4] is combined with the LAHET in order to construct a γ-ray source file from the collision information recorded on a LAHET

history file to calculate γ-production cross sections directly or for use as a source for HMCNP (a modification of MCNP 4A code) [10] for γ-transport calculations. Neutrons appearing in LAHET below 20MeV are written to a source file for transport with HMCNP. The photon source file generated by PHT may be merged with the neutron source file to provide a source for a coupled neutron/photon HMCNP run. We have to note that our present calculations do not include fission yields from fissions induced by neutrons bellow 20MeV in thick targets, and the yields estimated represent the lower limits of a complete fission process

The γ-ray output of PHT arises from two sources: from the decay of neutral pions and from the deexcitation of residual nuclei. For the latter, the assumption is made that all particle decay modes have been exhausted; thus γ-emission does not compete with particle emission. It is assumed that there exists a range of known energy levels, above which there is a continuum of energy levels with level density given by Gilbert-Cameron formulae [11]. The library of the level data contains over 50,000 listed levels. If the excitation energy of a residual nucleus lies between two levels, it is assigned randomly to one or the other of the levels with a probability that depends linearly on the distance from the levels. If the excitation is above the maximum known level, it is asssumed the level is in the continuum. The probability of a transition between levels is asssumed to be proportional to the Weisskopf single particle estimates [12] unless specified by the library. For levels in the continuum and for known levels with known spin and parity, a spin state is randomly assigned using the Gilbert-Cameron spin densities to generate a sampling distribution. For a transition within the continuum to a state of given spin, the transition probability is also proportional to the level density for the final spin state. The γ-cascade proceeds from the above assumptions. For an excitation energy lying in the continuum, transition to another level in the continuum competes with transitions to known levels. If the excitation energy lies within the known levels, or a level has been reached by transition from the continuum, the probability of a transition to lower levels is obtained from library data if available or from the model otherwise. When specified in the library data, a 0^+ to 0^+ transition is permitted to occur without γ-emission.

The input file for the PHT code was used with a "default" option, i.e. the full model is employed as described above. It is also possible to ignore the experimental branching ratios and perform a pure model calculations. The input cards for the LAHET code were chosen by changing the INC, the MPM and fission model parameters in order to reproduce existing experimental data. We will come back to the details later in this report.

3 Application of the LAHET code to residual nuclei (thin target)

A systematic survey on the capabilities to predict cross sections for the production of residual nuclides by medium-energy protons can be obtained from a recent International Model and Code Intercomparison for a large number of models and codes [13]. However, such an intercomparison cannot make in-depth analyses which have to be performed elsewhere. In this Chapter we compare in detail the experimental data with theoretical ones calculated by LAHET+PHT code as presented above in order to discuss its predictive capabilities.

It should be mentioned that the INC/EVAP model was created for applications as a particle generator for high-energy transport codes. Nevertheless, it has the advantages of energy- and momentum-, charge- and baryon-number conservation even in the case of residual nuclei. Although it is questionable whether Monte Carlo cascade calculations make accurate predictions for incident particle energies less than 100MeV, certain features of the isotope production can be understood, at least qualitatively, in terms of a prompt nuclear cascade followed by particle evaporation.

In our calculations we explored two INC models noted as "isabel" [14] and "bertini" [15]. The "default" option in all calculations stands for RAL evaporation-fission model [6], while in the rest of the cases, the ORNL evaporation-fission model [5] is employed. The choice of the multistage preequilibrium exciton model (MPM) [9] is defined by an "ipreq" input card (to be explained below).

The observed cross sections for production of Rb and Cs nuclei from 50MeV [16] and 156MeV [17] proton iduced reactions on a thin ^{238}U target are plotted in Figs. 1 through 4 along with the corresponding various model calculations. We found that the LAHET code is able to give a reasonable account of the trends in the observed data points in both the absolute values and the isotopic distributions. Surprisingly enough, even with 50MeV incident protons the predictions are quite good. However, we found that the choice of the fission model has to be selected very carefully. The ORNL fission medel, which has a non-zero fission probability only for residual nuclei (after the INC stage) with $Z \geq 91$, is strongly recommended in the case of uranium target. The RAL fission model, given as a "default" in the LAHET input, gives too broad isotopic distributions for all cases considered; it underestimates (by a factor of 2-4) the cross sections near the peak of the distribution but overestimates ones in the wings (by a factor of 10-100). The fission in uranium depends on the subactinide fission routines in

the RAL model, which are much less reliable than the actinide fission treatment in the ORNL.

In all cases, the choice of INC model ("bertini" or "isabel") does not greatly affect the calculated cross sections, and it is rather difficult to say which of them is more favourable in this respect. We will choose the "isabel" model later since it allows also deuterons as incident projectiles. A point should be made about the MPM model option. The preequilibrium model provides loss of both charge and excitation energy before the fission model is invoked and is expected to reduce the fission probability at higher energies. This effect is clearly seen if one compares the curves with "ipreq=1" (the MPM continues from the final state of the INC), "ipreq=0" (the MPM is not used) and "ipreq=3" (the MPM proceeds from the compound nucleus formed by absorption and the INC is used only to determine that an interaction has occured). In the case when the MPM is not used, the production of neutron-deficient isotopes is increased and better overall agreement with data is obtained. However, it appears that the more neutron-deficient isotopes are actually produced with greater rates than predicted both at lower and higher incident energies. The same tendency was observed after calculations of the Rb isotopic yields from a thick Nb target with 600MeV protons as shown in Figure 5. Since the LAHET is a Monte Carlo code, good statistical accuracy was achieved with available computer time only for production rates $\geq 10^8$ (atoms/s μA p); smaller yields do persist beyond this edge and can be estimated from extrapolation of the calculated values. However, for physics case, where very low production rates in the far tales of the distribution are of big relevance, only experimental values should be used at the moment. In our opinion, no model or extrapolation will give presently reliable values when the yields go down by more than 3 orders of magnitude.

4 Combined target (thick) for isotope production

In a charged particle induced cascade one can distinguish two qualitative physical regimes: a) a spallation driven, high energy phase and b) a neutron driven, fission dominated regime. Neutrons from the first phase are acting as a "source" for the second phase. The choice of the target materials for both of these physical regimes depends on the final purpose of such a device [18]. Most probably, the highest fission yields can be obtained from uranium fission reactions. If thermal, reactor,

and 14MeV neutron induced fissions are compared [19], it is suggested that more energetic neutrons give higher fission yields on the neutron deficient and/or rich sides by a factor of 10-100. For this reason a light metal target-converter as a high energy and forward peaked neutron source is chosen [3, 18].

We simulate a parallel deuteron beam which is uniformely distributed over an ellipse. A "default" source option of the LAHET in this case creates a "pencil beam" interacting with the combined target assembly as presented in Fig. 6. The target consists of a beam stopping beryllium cylinder (neutron source) with its radius r=3cm and a uranium cylinder (production target) with its radius r=4cm and length l=15cm. The production target is placed at 1cm distance from the beryllium target. Depending on the incident deuteron energy given by E_d=50MeV, 100MeV, and 200MeV we change the length of the stopping beryllium target accordingly, i.e. l=1cm, 3cm, and 10cm. In order to minimise the neutron loss from the system, and at the same time to provide it with some cooling conditions, the targets are surrounded by a cylindrical light water blanket with radius r=15cm (see Fig. 6). We tried three materials for the production target; a pure uranium ^{238}U with its density ρ=18.95g/cm^3, uranium dicarbide UC_2 with ρ=11.28g/cm^3, and uranium ^{238}U enriched by ^{235}U up to 80% with ρ=18.01g/cm^3.

Calculated total neutron multiplicities $\langle M_n \rangle$ in the case of thick targets are shown in Table 1. Neutron production in the beryllium target increases as a function of incident deuteron energy very sharply, i.e. a factor of 2 (or 4) increase in energy corresponds to a factor of 4 (or 10) increase in $\langle M_n \rangle$, and essentially to the increase of the range in the material. In this energy region, the beam intensity could not compensate neutron production at lower energies but the same beam power. Therefore, the highest 200MeV energy is suggested. In the secondary target neutron multiplicities are proportional to the number of neutrons in the primary one; we found that approximately 35-45% of all neutrons produced in the beryllium cross the surface of the secondary target, where neutrons are further multiplied by (n,xn) and (n,f) reactions. The energy spectrum of incoming neutrons is again very important in this process; more fissions and more (n,xn) reactions will occur for more energetic neutrons. Increase of secondary target density (factor 1.7 between UC_2 and U) resulted in a similar increment in neutron production (compare lines with UC_2 and U in Table 1).

In the fission of ^{238}U by reactor neutrons [19] the mass distribution of fission products contains two peaks located at A=95-105 and A=135-145. In between these two peaks at mass A=115-125 the distribution has its local minimum. For

a more detailed examination of isotope production in uranium by neutrons originating from the primary beryllium target we have chosen Rb (Z=37), Cd (Z=48) and Cs (Z=55) isotopes located within three regions of the mass distribution of fission products as mentioned above.

Our results with the UC_2 production target and three different incident energies of deuterons are shown in Fig. 7, where isotope yields are normalised per incident deuteron. As expected, higher incident energies resulted in broader isotope distributions (compare the curves with 50MeV and 200MeV deuterons, in particular). At the same time, at the very peaks of the distributions, increase in incident energy from 50MeV to 100MeV (to 200MeV) increased the isotope production by a factor of 8 (or 15). On the neutron rich (or deficient) side these differences are similar if extrapolated from presently calculated values.

We have also examined the isotope production as a function of target density as presented in Fig. 8. Again Rb, Cd and Cs isotopes were chosen. In this case we took 200MeV incident deuterons only. Dashed curves correspond to 100% ^{238}U as a secondary target with its density ρ=18.95g/cm^3, while solid curves stand for UC_2 with ρ=11.28g/cm^3. A factor 1.7 between the two densities gives a similar difference for isotope production per incident deuteron in favour of more densed material (a similar tendency was already observed for an in-target neutron production). If low density powders of UC_x are used in order to decrease the release time of isotopes, the yields given below have to be corrected by the ratio of the mean density, that is typically 1-2g/cm^3 for UC_x powders [20], over the corresponding density used in our calculations. In addition, the fact, that the UC_x system apparently moderates faster the neutron spectrum to below the threshold energy of ^{238}U fission, and/or effectively scatters neutrons out of the system, has to be taken into account.

For comparison in Fig. 8 we also included isotope production distributions (dotted curves) from thermal neutron induced fissions in 1g of the uranium ^{235}U [21]. The isotope rates are normalised per incident neutron per cm^2 in this case. Near the peaks of the mass distribution of fission products (also see examples with Rb and Cs in Fig. 8), the $n_{th}+^{235}U$ reactions give higher yields by 1-2 orders of magnitude. However, fission yields from high energy neutrons resulted in broader isotope distributions, what makes these two different methods equally efficient on the neutron deficient and/or neutron rich sides of the distributions. In addition, in the mass region A=115-125, where fission products from thermal neutron induced fissions exhibit their local minimum, high energy neutrons give higher fission yields by a factor of 10-20 (compare curves for Cd isotope distribution in Fig. 8).

More straightforward comparison of the two different methods discussed above is presented in Fig. 9, where one can easily see advantages/disadvantages these methods contain.

The use of highly enriched uranium for production of isotopes seems to be an interesting possibility too. In this context we investigated a sub-critical secondary target consisting of 20% ^{238}U and 80% ^{235}U with its averaged density ρ=18.01g/cm^3. Criticality calculation with the MCNP code [10] resulted in an effective neutron multiplication coefficient k_{eff} ~0.9 to be compared to k_{eff} ~0.1 in the case of a pure ^{238}U cylinder with the same geometry setup. In this particular case, we obtained 70 times more fissions* than in the target without ^{235}U. Correspondingly, a similar factor would result in the increase of the isotope production yields near the peaks of the fission products; even though all distributions would slightly be moved to the neutron deficient side (simply because $\frac{N}{Z}(^{235}\mathrm{U}) < \frac{N}{Z}(^{238}\mathrm{U})$). Such a target assembly, if considered, would allow to take advantages both of the thermal and high energy neutron induced fissions resulting in fission yields of the order of magnitude of 0.1 (atoms/d), i.e. even higher than in the case of the PIAFE project.

In order to compare the above proposed method for isotope production with the ones at already existing or planned experimental facilities we have chosen a number of isotopes given in Table 2. From Table 3 it is seen that both ISOLDE and SPIRAL-2 in-target isotope production rates (in atoms per sμAp) are very similar, while present GANIL fragmentation technique gives smaller values by a factor of 2-10. In the case of the PIAFE project, the isotope production is higher by 1-2 orders of magnitude, which corresponds to the fission yields expected for the sub-critical target assembly (80% ^{235}U) as described above.

However, for a realistic comparison of the different methods, it is important to take into account the efficiency of the ion-source, that may reduce considerably the final beam intensities. It is also very important to set realistic limits of the intensities of the primary beam currents. In our opinion, the UC_2 production target (r=4cm and l=15cm) would have similar total release-delay-source efficiencies as a typical ISOLDE target (r=1cm and l=20cm). We note that one has to correct the fission yields for the corresponding densities of different target materials as well. Hence, the final RIB intensities assuming expected total efficiency rates (see Table 2) and projected final incident beam intensities could be estimated from Table 3 for some of the isotopes.

*As a first approximation $N_{fiss} \sim k_{eff}/(1-k_{eff})$ [3], consequently the ratio of a number of fissions N_{fiss}(80% ^{235}U)/N_{fiss}(^{238}U)~81.

5 Beam heating and cooling of thick targets

It was mentioned above that a beryllium target-converter serves as an efficient neutron source for the isotope production by fissions in the secondary production target. It also decouples an intense charged particle beam from the secondary target in terms of the energy absorption and consequent target heating.

Calculated energy deposition rates in the combined target system (see Fig. 6) with 200MeV deuterons are given in Table 4. In the transport of particles with the LAHET code [4], ionization losses, inelastic and multiple Coulomb scattering as well as particle decay and nuclear excitation were taken into account. Fission heating from neutrons were tallied separately in order to compare it to the non-fission deposition rates for different target materials.

With incident beam power of 10kW, beryllium stopping target has to handle 8kW heat deposition (for example, at 50μA of incident deuteron beam intensity, 20MeV/d energy deposition rate corresponds to a heating rate of 1kW). As a consequence of the decoupling of beam stopping and isotope production targets, the heat deposited in UC_2 or ^{238}U is only of the order of 1kW and 1.7kW respectively. On the other hand, the highly enriched uranium target results in 50kW heat deposition mainly because of the increased number of fissions (see Table 4).

Unfortunately, the target systems of interest cannot through radioactive processes alone tolerate deuteron beam intensities beyond several μA. An analysis for conductive cooling (up to 8kW) by water-cooled channels was presented in [23]. Here we would like to describe another approach to conductive cooling, and give an example of a possible alternative target concept as initially proposed in Ref. [24]. This approach may be appealing in application to solid and liquid metal targets which exhibit high bulk density but require a limit on operating temperature.

Assuming a target operating temperature of 1000°C (1287°C and 1135°C are melting points of Be and U respectively) the following highly enriched uranium target configuration to conduct up to 60kW of deposited heat† to a water-cooled jacket is suggested (see Fig. 10). There are only a few materials with high (>1000°C) melting points and thermal conductivities k>1W/cm*K, including Be, Cu, Au and W. In our target geometry, if an inner target radius r_1=5cm and an outer radius r_2=12cm are assumed, about 952g/s water flow at inlet tempera-

†We recall that 10kW incident deuterons of 200MeV in the case of our combined target resulted in 8kW heat deposition in the primary beryllium target and up to 50kW heat deposition in the enriched uranium production target.

ture of 20°C and outlet temperature of 35°C is required to remove 60kW of heat deposited in target and not to exceed 1000°C on its surface. The temperature of the outer wall of the conducting material is about 493°C, and the temperature of the outer wall of the He gas annulus is about 75°C. Here thermal conductivities k_1=1.1W/cm*K and k_2=0.0033W/cm*K were chosen, and 0.026cm annular gap between the target body and a water cooling jacket was adopted (see Fig. 10 for details). Such a gaseous gap serves to insulate the water cooled jacket from the target chamber by providing a sharp temperature step in the conductive path. The target length of 15cm was kept as in the isotope production calculations. This analysis can easily be executed to address requirements that are more clearly defined in the context of a future specific primary/secondary target concept.

6 Conclusions

We estimated the neutron rich isotope production by neutron induced fissions in thick uranium targets. The stopping beryllium target-converter interacting with intermediate energy deuterons served as an efficient energetic neutron source. The total incident energy of the projectiles, the chosen geometry, density and atomic contents of the combined target assembly were the major parameters for the complete optimisation of high fission yields of our interest.

We found that, in the energy range from 50MeV to 200MeV of the incident deuterons, both the neutron and isotope production increases with beam energy for constant beam power. For this reason 200MeV (or higher energy) deuterons are suggested.

The increase of the secondary target density (a factor 1.7 between ^{238}U and UC_2) resulted in a similar increment both in neutron and isotope production yields. On the other hand, high material density will result in a less efficient isotope release from it. Similarly, for an in-target isotope production a small target volume is desirable, which would decrease the production yields proportionally to the decrease in a number of interactions. Depending on the isotopes of interest, the optimum target geometry, materials and mass density parameters have to be chosen.

The use of the uranium ^{235}U together with ^{238}U in the isotope production target seems to be a promising combination; we obtained 70 times more fissions by adding 80% of ^{235}U. A similar factor would result in the increase of the fission yields; and in the increase of the deposited heat. A conductive cooling presented

would be able to handle up to 60kW of the target heating in this particular example, where the increased number of fissions contribute more than 95% of the total thermal heat. In the case of the pure ^{238}U or UC_2 targets, 80% of the incident beam power is deposited in the primary Be target, and the heat dissipation issue is solved automatically in the production target.

In order to compare the different isotope production methods we have chosen GANIL, ISOLDE and PIAFE experimental facilities. By normalising corresponding in-target production rates for $6.25*10^{12}$ incident particles per second, we found that the above proposed method gives very similar in-target isotope production rates as the ISOLDE technique where 1GeV proton induced fissions on the thick uranium target are considered. The present GANIL fragmentation method gives smaller values by a factor of 2-10, while the PIAFE project, based on thermal neutron induced fissions on ^{235}U, results in the fission yields by 1-2 orders of magnitude higher/lower for different fission yields. However, for a more realistic comparison it is very important to take into account the final release-delay-source efficiencies, which might be different for different methods as well as the available primary beam intensities.

Anyhow, the SPIRAL Phase-II project with the isotope production by neutron induced fissions following the Be(d,xn) reactions is a very interesting possibility. Even with 6kW deuteron beam at 200MeV (compatible with the existing characteristics of GANIL) we expect a 2-3 orders of magnitude increase in the final secondary beam intensity for some isotopes estimated from present fragmentation of the target and/or the heavy ion beam.

7 Acknowledgments

We wish to express our appreciation to R.E. Prael for providing us with the LAHET code system. We also would like to thank J.A. Nolen for fruitful discussions and comments at different stages of this manuscript.

References

[1] J.A. Nolen, Proceedings of the Third International Conference on RNB, Gif-sur-Yvette, France, 24-27 May 1993, Ed. D.J. Morrissey, Editions Frontiers (1993) 111; and Concept for Advanced Exotic Beam Facility Based on ATLAS, Argonne National Laboratory (February 1995)

[2] D. Ridikas and W. Mittig, GANIL preprint **P 97 19**, GANIL, Caen (May 1997); available from CERN Library Catalogue at "http://alice.cern.ch/"

[3] D. Ridikas and W. Mittig, GANIL preprint **P 98 2**, GANIL, Caen (February 1998); available from CERN Library Catalogue at "http://alice.cern.ch/"

[4] R.E. Prael and H. Lichtenstein, "User Guide to LCS: The LAHET Code System," Los Alamos National Laboratory Report LA-UR-89-3014 (September 1989)

[5] J. Barish *et al.*, ORNL/TM-7882, Oak Ridge National Laboratory (July 1981)

[6] F. Atchison, "Spallation and Fission in Heavy Metal Nuclei under Medium Energy Proton Bombardment" in "Targets for Neutron Beam Spallation Sources", Jül-Conf-34, Kernforschungsanlage Jülich GmbH (January 1980)

[7] L. Dresner, ORNL/TM-196, Oak Ridge National Laboratory (April 1962)

[8] D.J. Brenner, R.E. Prael, J.F. Discello and M. Zaider, "Improved Calculations of Energy Depostion from Fast Neutrons", in Proceedings Fourth Symposium on Neutron Dosimetry, EUR-7448, Munich-Neuherberg (1981)

[9] R.E. Prael and M. Bozoian, LA-UR-88-3238, Los Alamos National Laboratory (September 1988)

[10] Group X-6, "A General Monte Carlo Code for Neutron and Photon Transport", LA-7396-M, Los Alamos National Laboratory (April 1981)

[11] A. Gilbert and A.G.W. Cameron, Can. Journ. of Phys. **43** (1965) 1446

[12] J.M. Blatt and V.F. Weisskopf, Theoretical Nuclear Physics, John Wiley, New York (1952)

[13] R. Michel and P. Nagel, International Codes and Model Intercomparison for Intermediate Energy Activation Yields, NEA/OECD, NSC/DOC(97)-1 (1997)

[14] Y. Yariv and Z. Fraenkel, Phys. Rev. **C 20** (1979) 2227

[15] H.W. Bertini, Phys. Rev. **188** (1969) 1711

[16] B.L. Tracy *et al.*, Phys. Rev. **C 5** (1972) 222

[17] J. Chaumont, PhD thesis, CNRS, Orsay (1970) unpublished

[18] D. Ridikas and W.Mittig, Proceedings of the 2nd International Conference on Exotic Nuclei and Atomic Masses (ENAM'98), Shanty Creek Resort, Bellaire, Michigan, USA, 23-27 May 1998 (to be published)

[19] V. K. Rao *et al.*, Phys. Rev. **C 19** (1979) 1372

[20] A.E.Barzakh *et al.*, Nucl. Instr. & Meth. **B 126** (1997) 150; V.I. Tikhonov, private communication (April 1998)

[21] PIAFE Collaboration, Piafe Project: Physics Case, SARA/ISN, Institute des Sciences Nucléaires de Grenoble (June 1994)

[22] H.L. Ravn *et al.*, Nucl. Instr. & Meth. **B 88** (1994) 441

[23] T. W. Eaton, H.L. Ravn and the ISOLDE Collaboration, Nucl. Instr. & Meth. **B 26** (1987) 190

[24] W.L. Talbert, H.H. Hsu and F.C. Prenger, Nucl. Instr. & Meth. **B 70** (1992) 175

	50MeV	100MeV	200MeV
in ^{9}Be	0.083	0.318	0.993
in UC_2	0.022	0.182	0.612
in U	0.032	0.285	0.967

Table 1: In-target neutron production with incident 50MeV, 100MeV, and 200MeV deuterons on Be+UC_2 and Be+U target systems (see Fig. 6). In all cases neutron multiplicities $\langle M_n \rangle$ are normalised per incident deuteron.

Isotope	Half-life	Production rate LAHET (atoms/d)	Efficiency ISOLDE (%)	Efficiency PIAFE (%)
$^{72}_{30}$Zn	46h	$1.4*10^{-5}$	8	
$^{91}_{36}$Kr	8.6s	$5.9*10^{-4}$	29	28
$^{94}_{36}$Kr	0.2s	$2.1*10^{-4}$	6.4	0.4
$^{97}_{37}$Rb	0.17s	$2.2*10^{-4}$	11	5.7
$^{132}_{50}$Sn	40s	$4.8*10^{-5}$	2.4	0.36
$^{142}_{54}$Xe	1.22s	$4.1*10^{-5}$	26	12
$^{144}_{55}$Cs	1s	$1.6*10^{-4}$	38	12

Table 2: Estimate of the in-target production of the radioactive elements from xn+UC_2, where neutrons were originating from 200MeV d+Be stopping target (see text and Fig. 6 for details). The final expected release-delay-source efficiencies are from [22].

Beam	ISOLDE at./sμA p	GANIL at./sμA p	PIAFE at./(s 6.25*10^{12} n/s cm^2)	SPIRAL-2 at./sμA p
$^{72}_{30}$Zn	2.8*10^9	3.3*10^8		0.9*10^8
$^{91}_{36}$Kr	4.1*10^9	5.8*10^8	2.6*10^{11}	3.7*10^9
$^{94}_{36}$Kr	1.7*10^8	4.9*10^7	8.8*10^9	1.3*10^8
$^{97}_{37}$Rb	8.7*10^8	4.6*10^8	4.6*10^9	1.4*10^9
$^{132}_{50}$Sn	1.5*10^8	2.6*10^7	5.4*10^{10}	3.0*10^8
$^{142}_{54}$Xe	1.3*10^8	2.3*10^7	4.1*10^{10}	2.6*10^8
$^{144}_{55}$Cs	2.2*10^{10}	3.9*10^9	3.4*10^{10}	1.0*10^9

Table 3: Estimate of projected in-target isotope production of RIB (the numbers for ISOLDE, GANIL and PIAFE facilities are taken from [22]). The lists of beam intensities are normalised to a primary beam intensity of one particle μA, except for the thermal neutron based PIAFE facility for which neutron flux densities of 6.25*10^{12} n/s cm^2 have been considered. Final beam intensities assuming expected efficiencies (see Table 2) and the projected primary currents of p:100μA, ^{12}C:8μA, n:10^{14}/s cm^2 and d:50μA at ISOLDE, GANIL, PIAFE and SPIRAL-2 experimental facilities respectively can be estimated. See text and Ref. [22] for details concerning the different target geometries and materials in the case of different experimental facilities.

Target	Density (g/cm^3)	Total energy deposition (MeV/d)	Fission contribution (%)
^{9}Be	1.848	160.4	0.0
UC_2	11.28	18.3	30
^{238}U	18.95	33.7	40
U(80% ^{235}U)	18.01	1010.6	97

Table 4: In-target energy deposition rates for 200MeV deuterons.

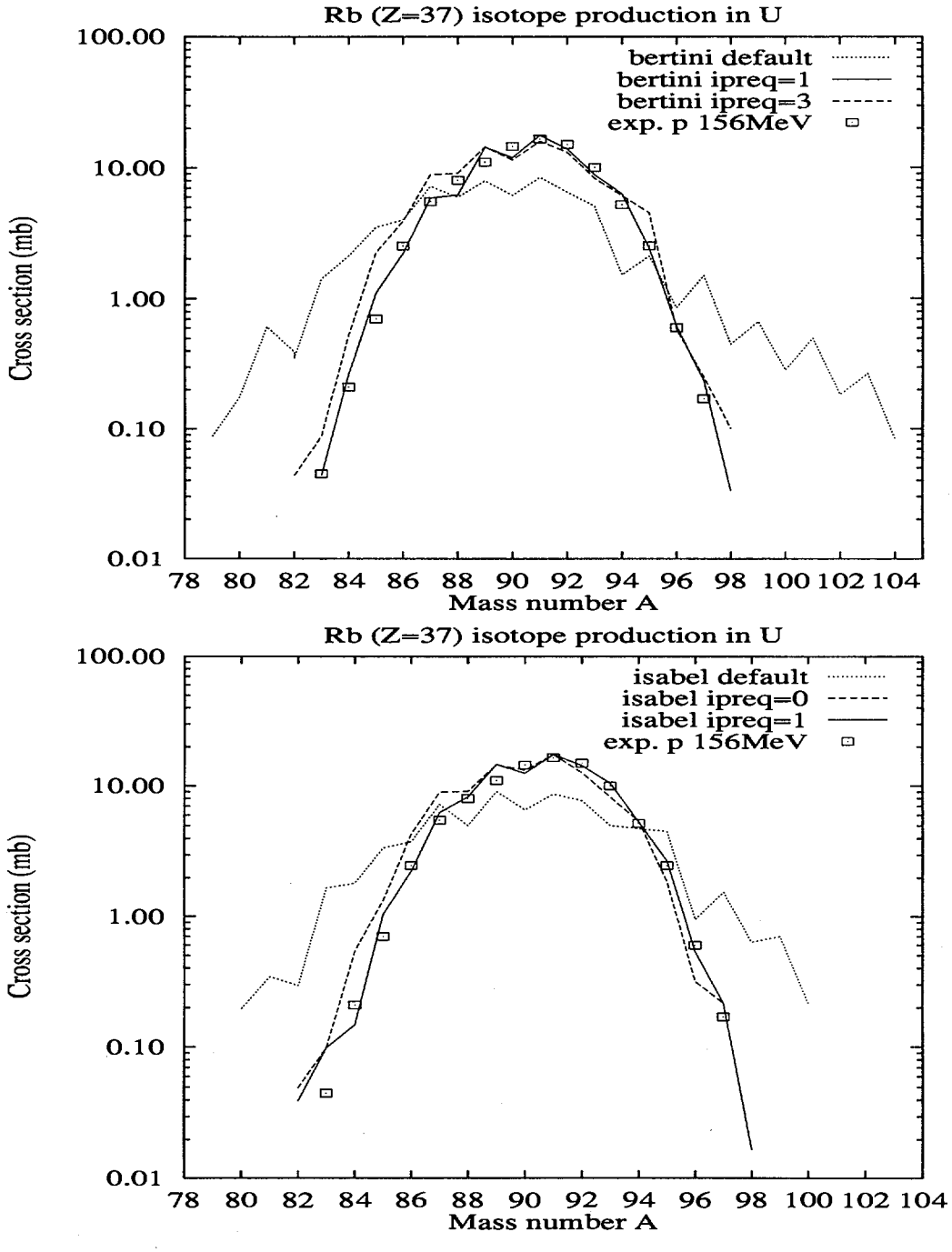

Figure 1: Isotopic distributions of Rb in the system of 156MeV p+^{238}U.

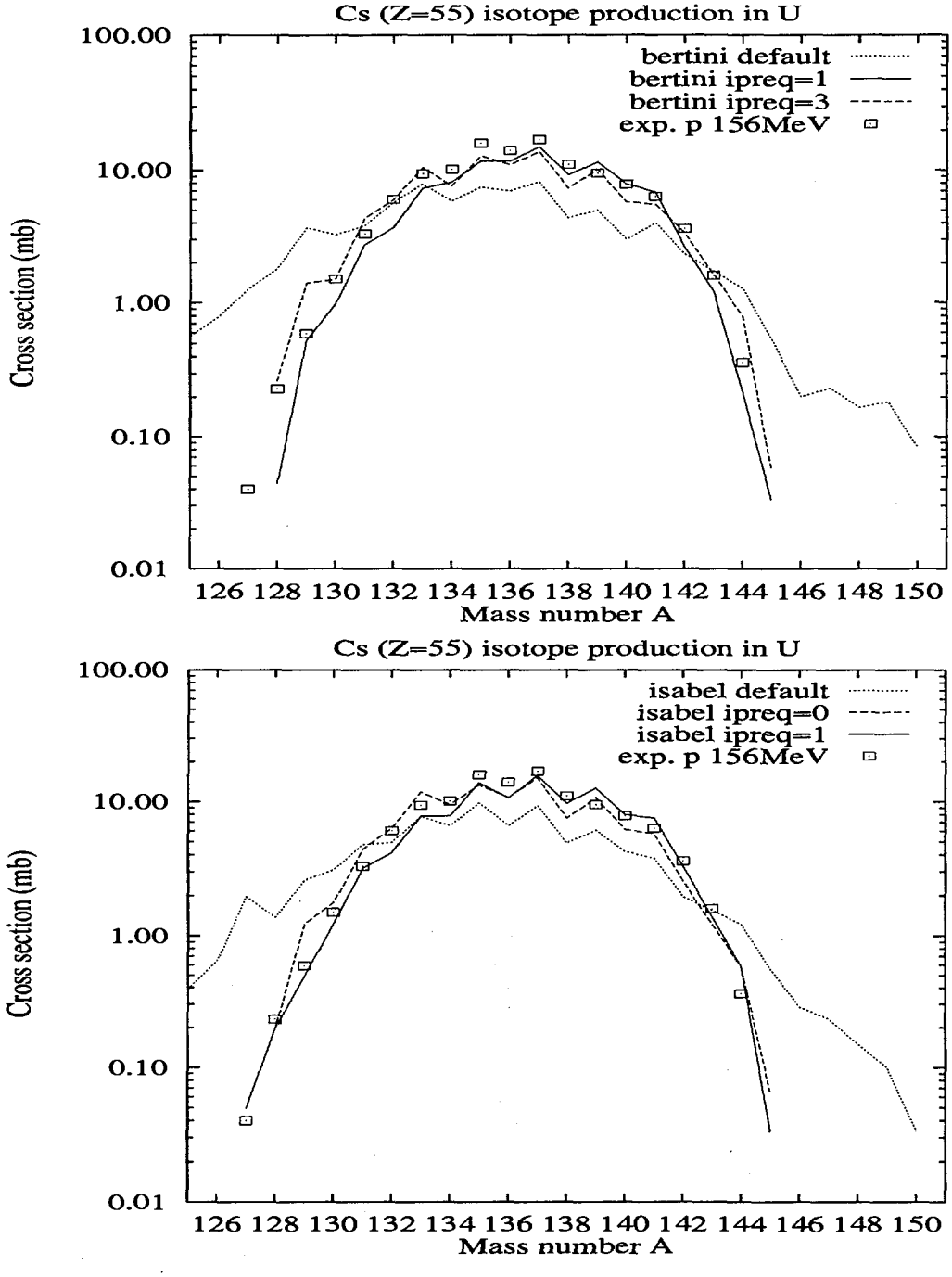

Figure 2: Isotopic distributions of Cs in the system of 156MeV p+^{238}U.

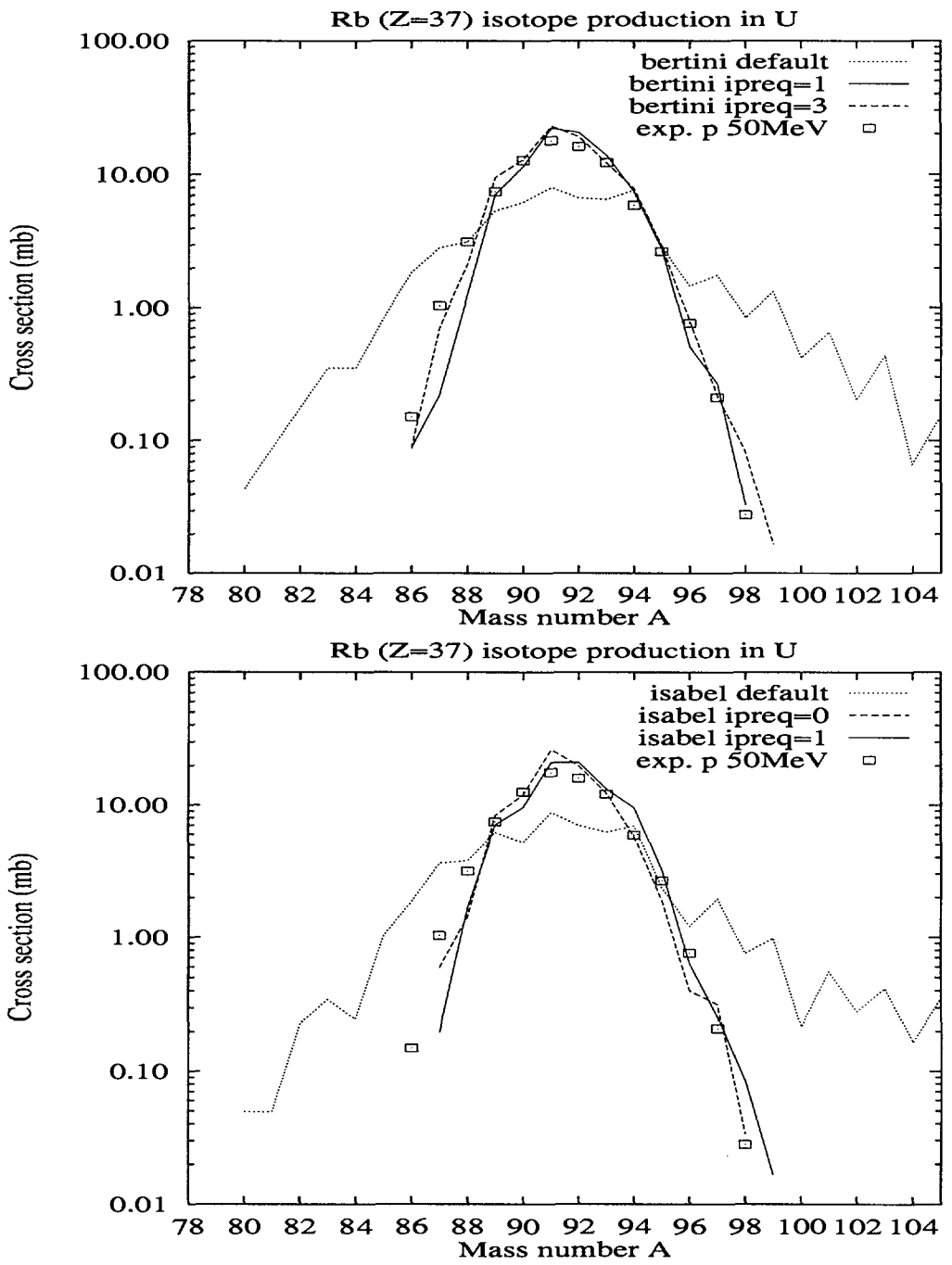

Figure 3: Isotopic distributions of Rb in the system of 50MeV p+^{238}U.

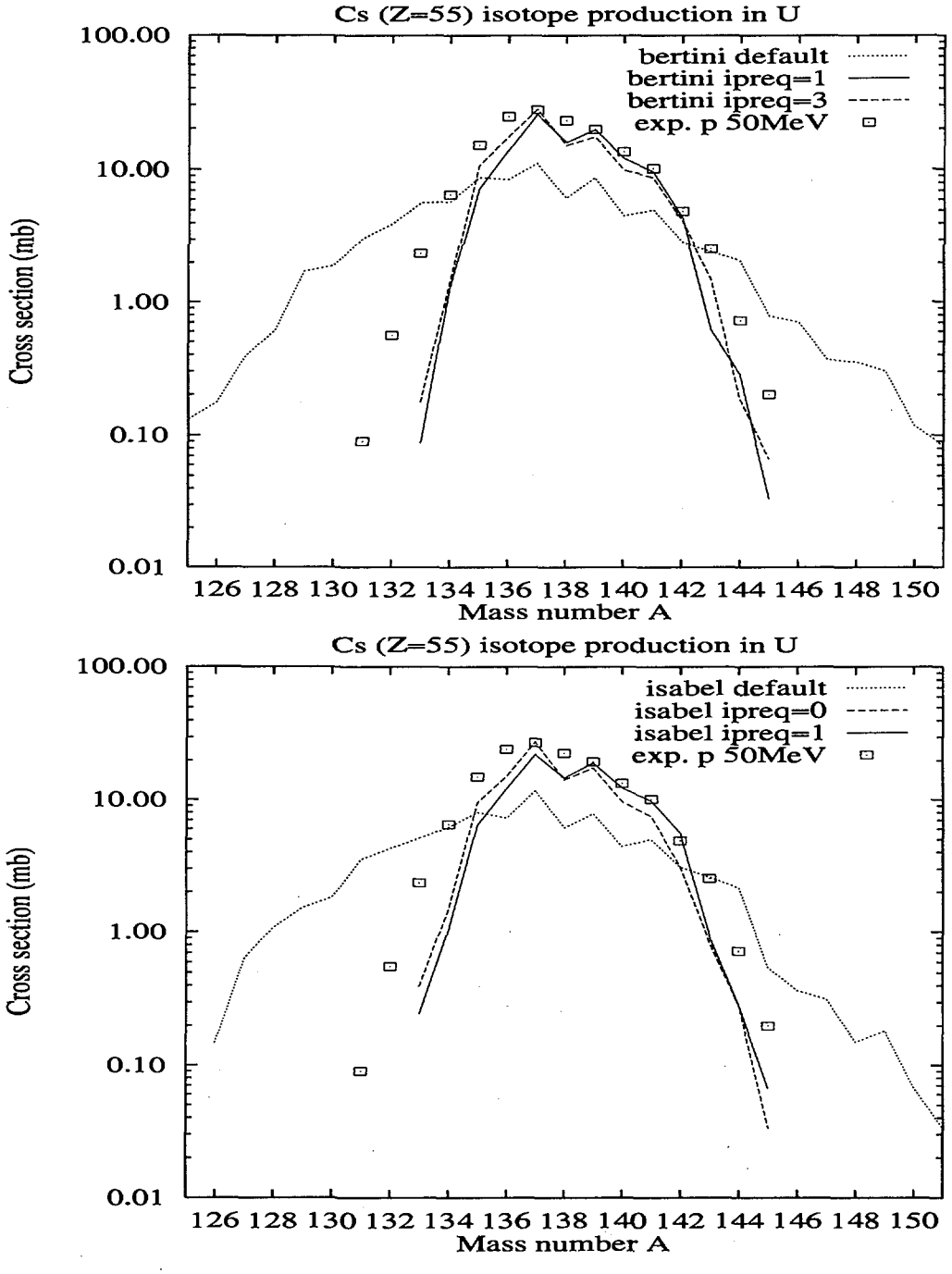

Figure 4: Isotopic distributions of Cs in the system of 50MeV p+^{238}U.

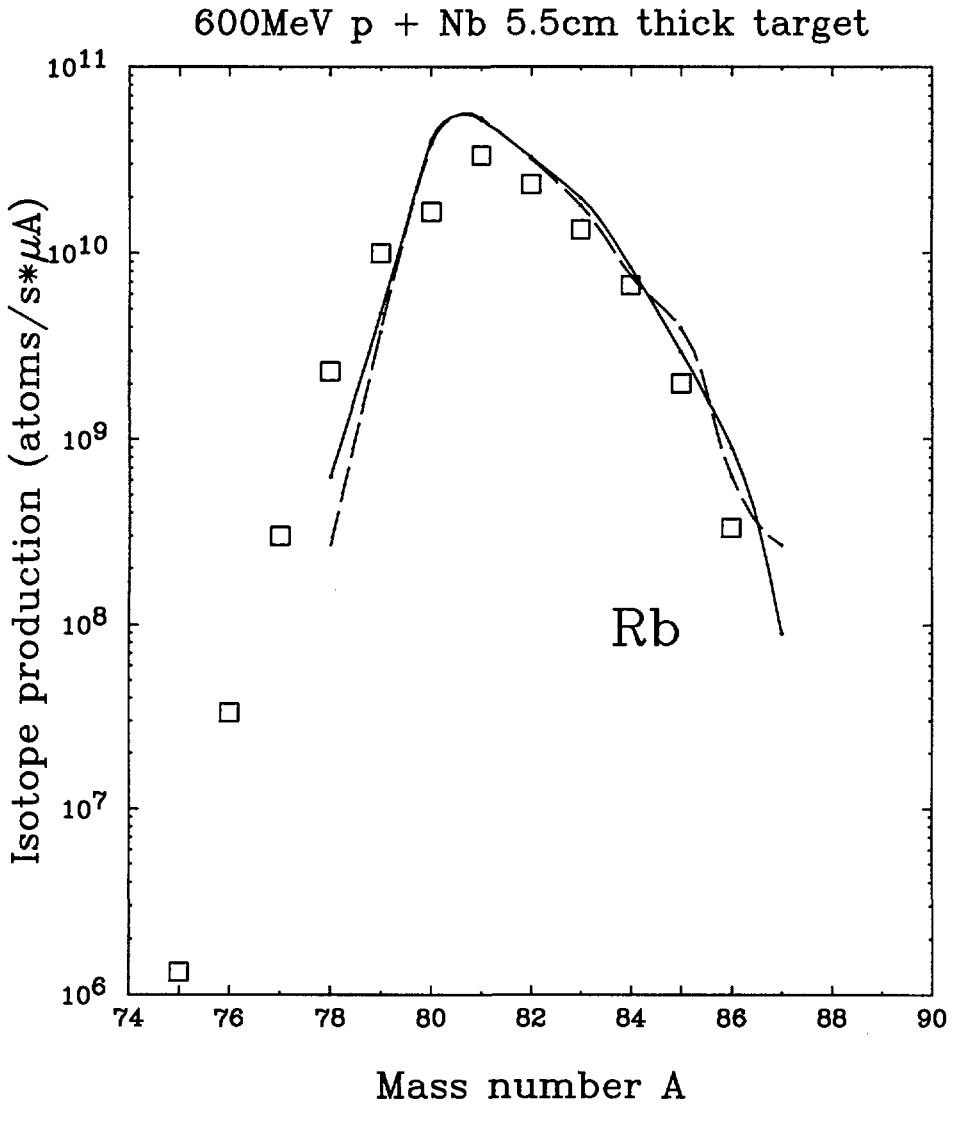

Figure 5: Comparison of measured [22] and predicted Rb isotope production rates for 600 MeV protons interacting with 5.5 cm thick Nb target. Dashed curve corresponds to the "default" input for the ISABEL intranuclear cascade (INC) without the multistep preequilibrium model (MPM), while the solid curve represents ISABEL INC+MPM model calculations.

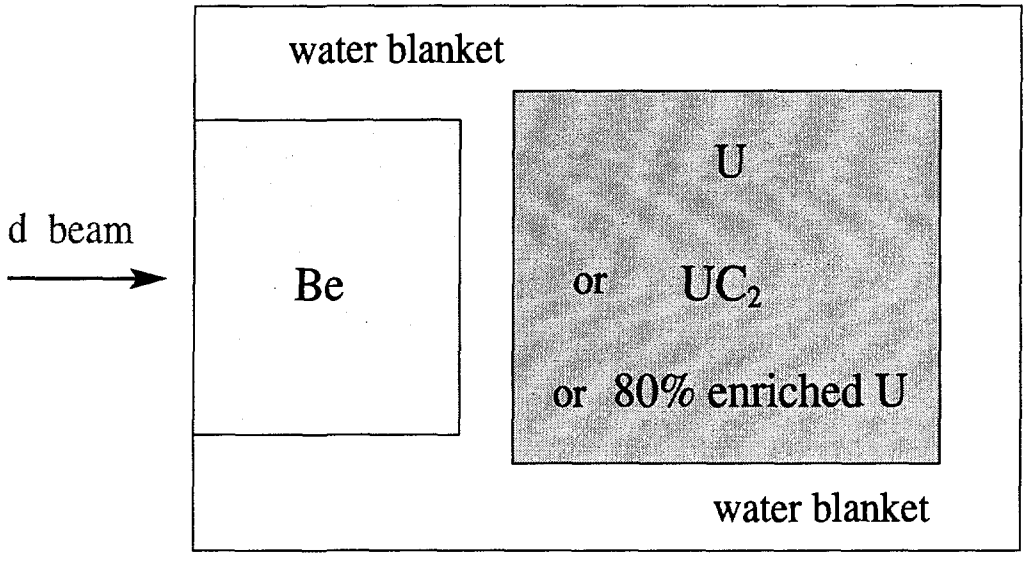

Figure 6: A combined target assembly for neutron multiplication and isotope production with incident deuterons. The target system is symmetric with respect to the beam axis.

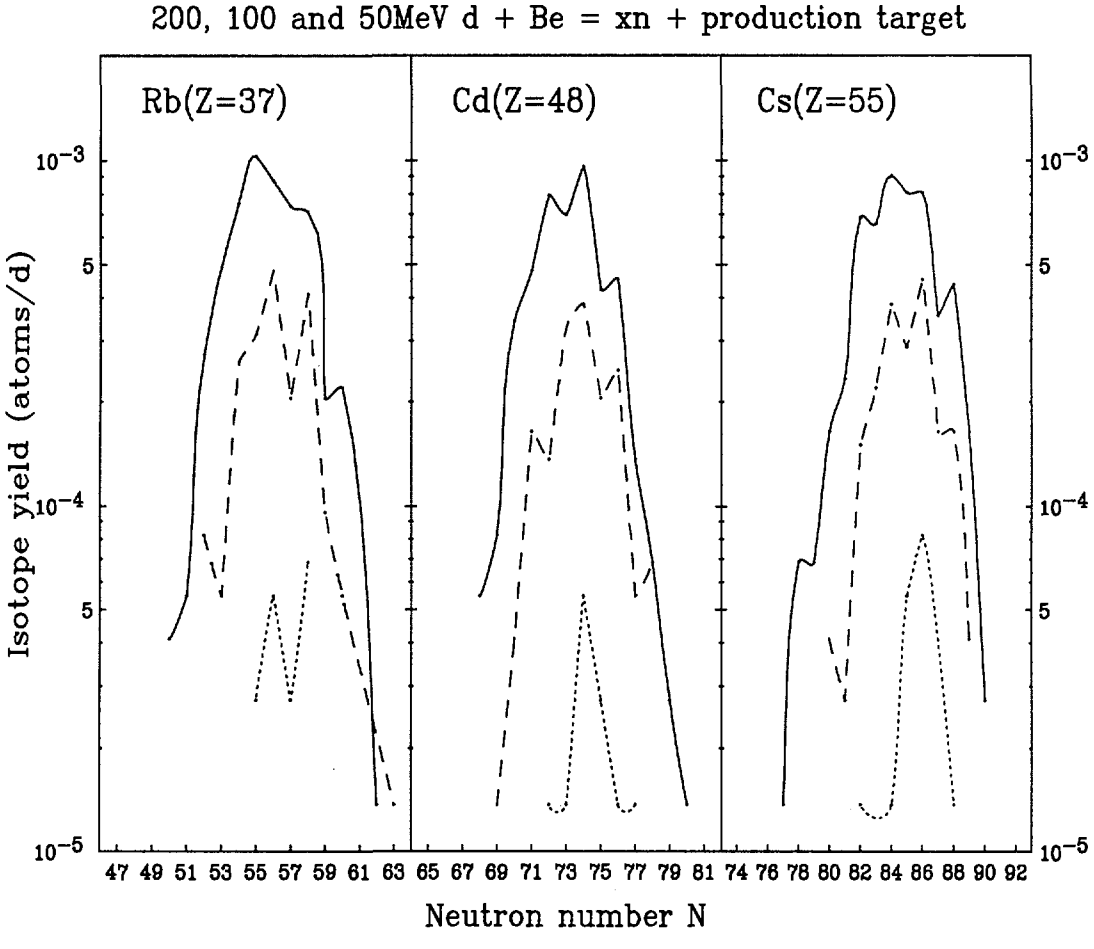

Figure 7: Isotopic distributions of the in-target production of Rb, Cd and Cs in the system of 50MeV (dotted curve), 100MeV (dashed curve) and 200MeV (solid curve) d+Be $\rightarrow$ xn+UC_2 (see Fig. 6).

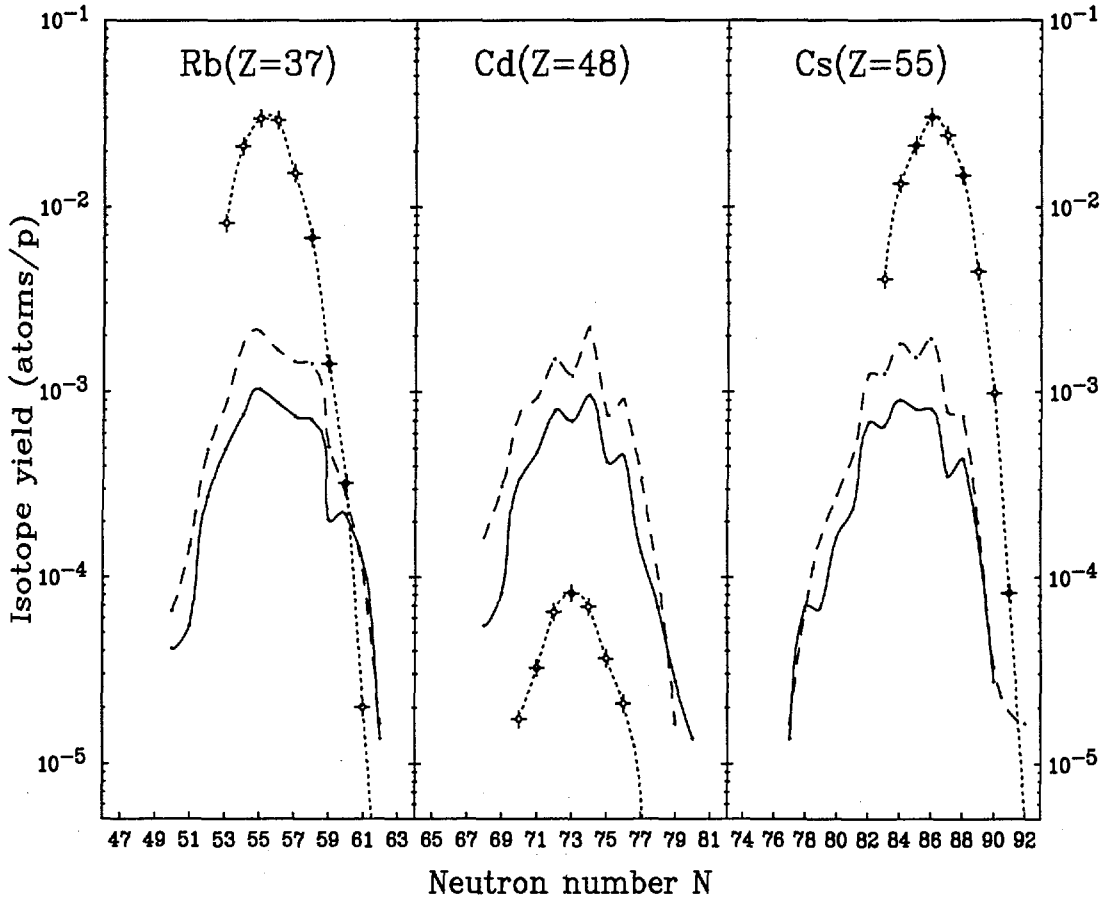

Figure 8: Isotopic distributions of the in-target production of Rb, Cd and Cs in the systems of 200MeV d+Be $\rightarrow$ xn+UC_2 (solid curves in atoms per deuteron), 200MeV d+Be $\rightarrow$ xn+U (dashed curves in atoms per deuteron) (see Fig. 6), and n_{th}+^{235}U (dotted curves in atoms per neutron/cm^2) as from [21].

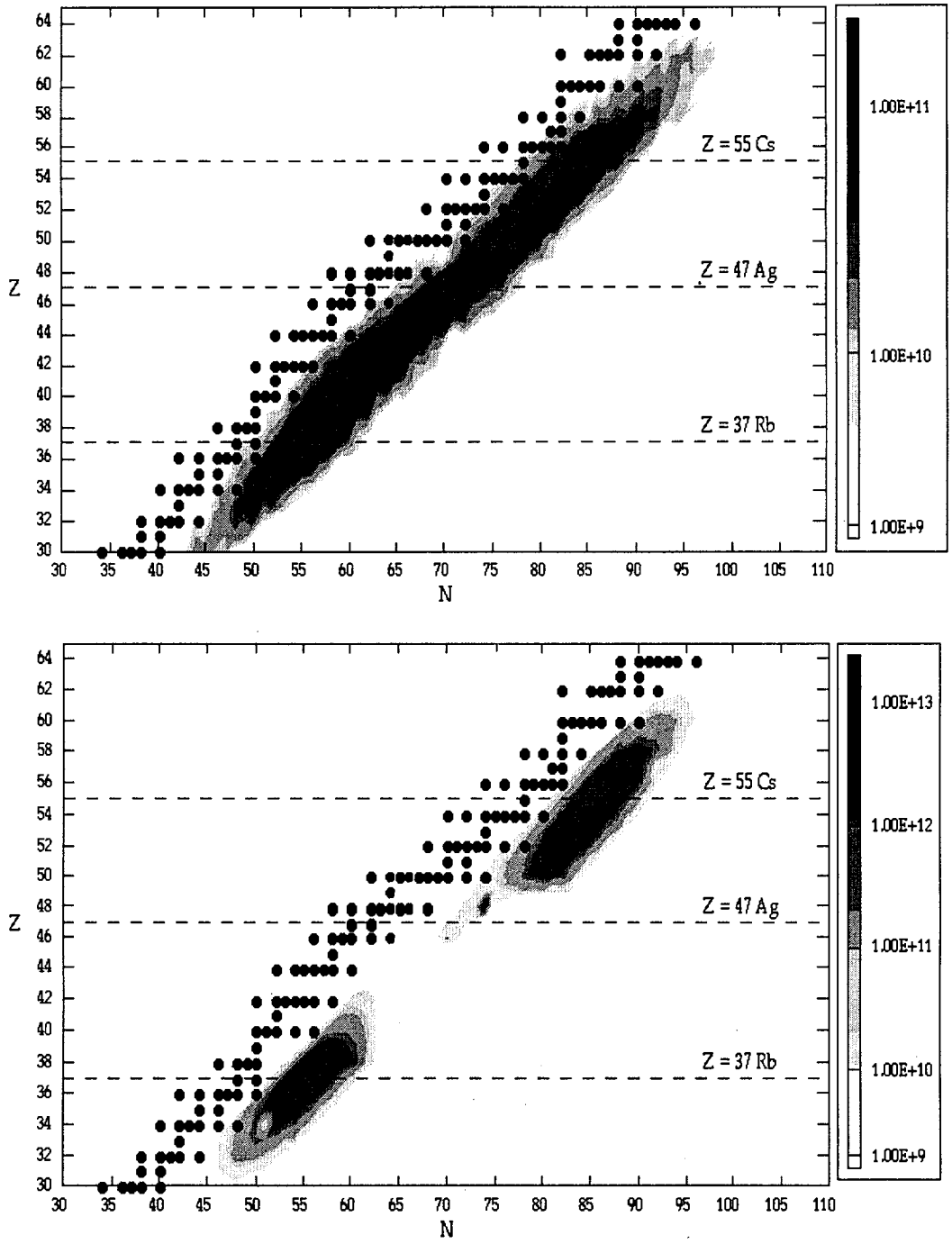

Figure 9: Comparison of fission yields in the case of 200MeV d+Be→xn+^{238}U normalised for 1.9*10^{14}(d/s) (upper part) versus n_{th}+^{235}U as from [21] normalised for 1.9*10^{14}(n/s cm^2) (lower part).

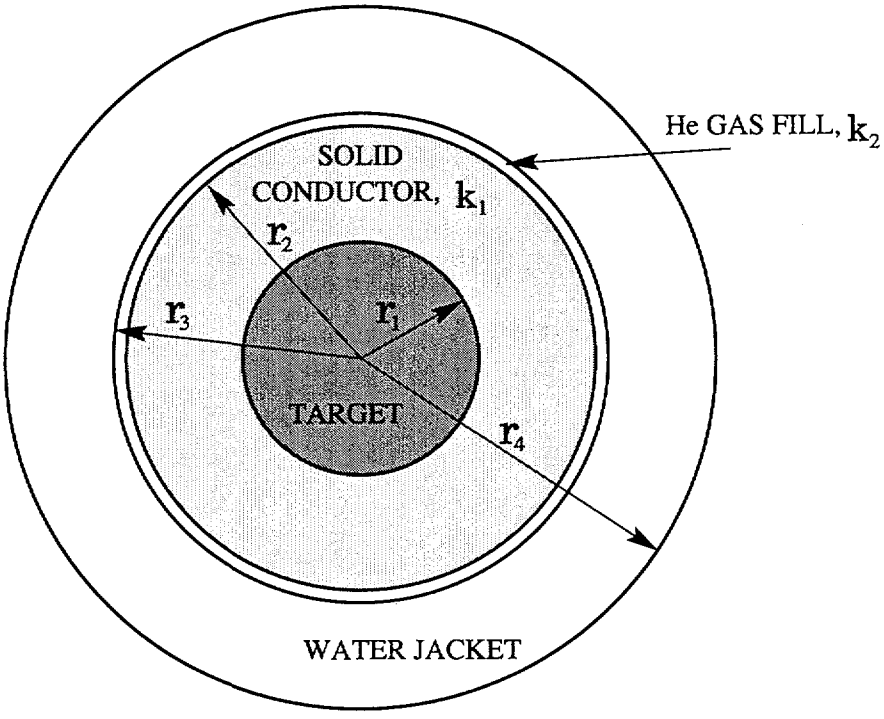

Figure 10: Conductive target cooling system in its cross-sectional view (see text and Ref. [24] for details).